ENVIRONMENTAL SCIENCES 2001 Vol. 10, No. S-4, 197~206
Bulletin of the Korean Environmental Sciences Society

Long-range Transport Mechanisms of Asian Dust associated with the Synoptic Weather System

Yoo-Keun Kim, Hwa-Woon Lee, Yun-Seob Moon*, and Sang-Keun Song

Department of Atmospheric Sciences, Pusan National University, Busan, Korea
**Department of Physics, University of Toronto, Toronto, Canada*

(Manuscript received on November 27, 2001)

The long-range transport mechanisms of Asian dust were analyzed based on the synoptic weather system and numerical simulation by using NCEP/NCAR reanalysis and TOMS data during the periods of 1996-2001. We classified the whole weather types of eastern Asia during spring and created the representative weather types during the yellow sand events using cluster analysis and weather charts for the last 6 years(1996~2001). These long-range transport mechanisms were related to various pressure patterns including high and low, trough and ridge, and upper-level fronts.

Case studies of the yellow sand events have performed by the simulation of MM5 with meteorological elements such as the horizontal wind of u and v component, potential temperature, potential vorticity, and vertical circulation during the episodic days(2~8 March 2001). In addition, the origin of the long-range transport was examined with the estimation of backward trajectory using HYSPLIT4 Model.

In this paper, we concluded that three weather types at 1000 hPa, 850 hPa, 500 hPa, and 300 hPa levels were classified respectively. The dominant features were the extending continental outflow from China to Korea at 1000 hPa and 850 hPa levels, the deep trough passage and cold advection at 500 hPa and 300 hPa levels during the yellow sand events. And also, we confirmed the existence of polar/subtropical jets in the upper-level, the behavior of potential vorticity over Korea, the estimation of potential vorticity through vertical cross section, and the transport of yellow sand through backward trajectories.

Key words : yellow sand, long-range transport, synoptic weather system, cluster analysis, weather types, potential vorticity

1. Introduction

The long-range transport of air pollutants including Asian dust is generally explained by the circulation and advection of wind in the atmosphere. Analyzing the characteristics of the long-range transport of dusts on an episode(or high concentration) day is one of the key elements in distinguishing the origin of Asian dust and analyzing the distribution of air pollution. In fact, the long-range transport mechanism and the optical properties of Asian dust, or known as Yellow sand, have been studied using ground-based instruments such as lidar, a sun photometer, sky radiometer, and an optical particle counter(OPC) in the last two decades[1~4].

Asian dust is quite different from that in other regions of the world. It originates mainly from the arid region at high altitude(1~2 km or higher) in central and eastern China, such as Takla-Makan, Gobi, and Ordos deserts, Loess and Shan plateaus. It is easily delivered into the free troposphere and then transported thousands of kilometers downwind over Korea, Japan, and even over the Pacific Ocean during the spring[5~7]. These dust are initiated by the strong westerly winds and travel behind cold fronts, which occur most frequently during March, April, and May when the arid region is not covered by vegetation.

Numerical modeling plays an important role in

understanding the transport mechanism of dusts. Intensive modeling studies have already been conducted to examine the transport of Saharan dusts and its impact on global radiation budget[8~10]. Several numerical modeling studies[11~13] have been carried out to investigated Asian dust transport.

Many attempts have been made to analyze the long-range transport path of the yellow sand events in the atmosphere by using the aerosols and meteorological data, and simulate the life cycle of soil dust by using general circulation models (GCMs)[14~15]. Such approaches helped us to investigate the effects of desert dusts on climate at a global scale. However, it is difficult to analyze and apply this modeled transport path to regional scale environmental problems continuously due to the limited observational data available.

This study focuses on the specific studies of the yellow sand events associated with the synoptic weather system and the strong meandering streams (or jet streams). The first purpose is to analyze the weather types of eastern Asia in springtime and to create the representative weather types during the yellow sand events associated with the strong meandering streams by using the meteorological data and weather charts for the last 6 years(1996~2001). The second is to clarify the mechanisms and origin of the long-range transport of yellow sand by using Mesoscale Meteorological Model 5(MM5), Read/Interpolate/Plot(RIP), and HYbrid Single-Particle Lagrangian Integrated Trajectory Model 4(HYSPLIT4) in eastern Asia.

2. Data and methods

The specific mechanisms and weather types in the yellow sand events are examined by using the meteorological data including National Centers for Environmental Prediction/National Center for Atmospheric Research(NCEP/NCAR) reanalysis data and aerosol index of Total Ozone Mapping Spectrometer(TOMS) data in eastern Asia for the last 6 years(1996~2001). Then, we classified the whole weather types of eastern Asia in springtime and created the representative weather types during the yellow sand events by using cluster analysis and weather charts for the last 6 years(1996~2001). In addition, case studies of the yellow sand events using MM5 and RIP program were performed to verify the mechanisms of the long-range transport of yellow sand from China to Korea. We simulated the meteorological elements such as the horizontal wind of u and v component, potential temperature, potential vorticity, and vertical circulation during the study period. The origin of the long-range transport of yellow sand was also clarified with the estimation of back trajectory using HYSPLIT4 Model.

3. The analysis of the weather types over eastern Asia in springtime

3.1. The classification of the weather types using cluster analysis

Meteorological parameters such as geopotential height, air temperature, potential temperature, u and v components of wind, and potential vorticity were first selected along the isobaric surface(1000 hPa, 850 hPa, 500 hPa, and 300 hPa levels) to classify the whole weather types during the study period(1996~2001) by using cluster analysis (Table 1). In this study, we divided 4 levels to understand the spatial and temporal distribution of the synoptic weather system, and the results of cluster analysis on the isobaric surface were shown in Table 2. All meteorological parameters used cluster analysis were statistically significant at the 5% confidence level along the isobaric surface, and especially wind fields and geopotential heights were highly significant.

The whole weather types of eastern Asia were obtained from the findings of cluster analysis (SPSS, Inc.). The weather types were determined only when all the patterns of each isobaric surface were vertically coincided. Three weather types were classified at 1000 hPa, 850 hPa, 500 hPa, and 300 hPa levels respectively(Table 3). The weather types of each isobaric surface obtained from cluster analysis were similar to those from weather chart analyses, although there was a little difference between them in detail. But, it is thought that the whole weather types classified by two methods must reveal the characteristics of surface high and low-pressure systems, upper-level troughs, and cold advections in springtime.

Table 1. Meteorological parameters for cluster analysis

Variable	Content	Unit
H300	300 hPa geopotential height	m
H500	500 hPa geopotential height	m
H850	850 hPa geopotential height	m
H1000	1000 hPa geopotential height	m
T300	300 hPa air temperature	℃
T500	500 hPa air temperature	℃
T850	850 hPa air temperature	℃
T1000	1000 hPa air temperature	℃
θ 300	300 hPa potential temperature	K
θ 500	500 hPa potential temperature	K
θ 850	850 hPa potential temperature	K
θ 1000	1000 hPa potential temperature	K
U300	300 hPa zonal wind velocity	m s^{-1}
U500	500 hPa zonal wind velocity	m s^{-1}
U850	850 hPa zonal wind velocity	m s^{-1}
U1000	1000 hPa zonal wind velocity	m s^{-1}
V300	300 hPa meridional wind velocity	m s^{-1}
V500	500 hPa meridional wind velocity	m s^{-1}
V850	850 hPa meridional wind velocity	m s^{-1}
V1000	1000 hPa meridional wind velocity	m s^{-1}
PV300	300 hPa potential vorticity	PVU (10^{-6} m^2 s^{-1} K kg^{-1})
PV500	500 hPa potential vorticity	PVU (10^{-6} m^2 s^{-1} K kg^{-1})
PV850	850 hPa potential vorticity	PVU (10^{-6} m^2 s^{-1} K kg^{-1})
PV1000	1000 hPa potential vorticity	PVU (10^{-6} m^2 s^{-1} K kg^{-1})

Table 2. The occurrence number of each cluster in springtime for the last 6 years(1996~2001)

	1000 hPa	850 hPa	500 hPa	300 hPa
Cluster 1	168.000	158.000	253.000	138.000
Cluster 2	208.000	298.000	164.000	273.000
Cluster 3	176.000	96.000	135.000	141.000
Valid	552.000	552.000	552.000	552.000
Missing	0.000	0.000	0.000	0.000

Table 3. The classification of the whole weather types in eastern Asia in springtime

Cluster	Weather type
1000 hPa/cluster 1	Low-pressure cell passage and extended continental anticyclone following a cold front to Korea
1000 hPa/cluster 2	Traveling anticyclone to Korea and high-pressure cell within eastern Asia
1000 hPa/cluster 3	Low-pressure cell passage near Korea
850 hPa/cluster 1	Low-pressure cell passage and extended continental anticyclone to Korea
850 hPa/cluster 2	Traveling anticyclone to Korea and high-pressure cell within eastern Asia
850 hPa/cluster 3	Low-pressure cell passage near Korea
500 hPa/cluster 1	Trough (or low-pressure cell) in the east of China and ridge in Korea
500 hPa/cluster 2	Upper-level trough passage and cold advection at the northwestern/north of Korea
500 hPa/cluster 3	Zonal flow of geopotential heights with no trough and ridge
300 hPa/cluster 1	Trough (or low-pressure cell) in China and ridge in west of Korea
300 hPa/cluster 2	Upper-level trough passage and cold advection at the north of Korea
300 hPa/cluster 3	Zonal flow of geopotential heights with no trough and ridge

3.2. Analysis of the weather types during the yellow sand events

3.2.1. Concepts of the weather types associated with the yellow sand events

The thermal cyclone may occur in the large area of Gobi desert and the eastern China with a high sensible heat flux caused by solar heating. In the typical wavetrain of the baroclinic westerlies aloft, there is cyclonic vorticity advection(CVA) downstream from the maxima in absolute vorticity, which are located along trough axes. Vorticity advection is more cyclonic with height because the advection at the upper level is stronger than the surface. Thus there is rising motion downstream from upper-level troughs. The effect of differential vorticity advection makes the surface pressure fall, and hence contribute to the formation of a surface cyclone or trough. Similarly, downstream from a ridge aloft, the effect of differential vorticity advection is to make the surface pressure rise and contribute to the formation of a surface anticyclone or ridge[16].

Thus the air parcel in the China inland can move up and down by means of the synoptic weather system such as the surface high and low-pressure systems, the upper-level ridge and trough. It is traveling toward Korea along westerlies. At the same time, the surface high and low-pressure systems following the upper-level trough and cold front can form in the vicinity of Korea, and this low-pressure system accompanying with cold and warm front plays a role in blocking the flow of wind. Thus this dust-rich air parcel entering from China may transport to Korea and intrude into the lower troposphere because of stratosphere-troposphere exchange(STE) associated with these meteorological forces and the strong meandering streams of the upper troposphere.

3.2.2. Characteristics of the weather types

Both the cluster analysis and weather charts of Japan Meteorological Agency(JMA) have been applied to classify the representative weather types associated with the yellow sand events by using the selected upper air data. The weather types presented on the yellow sand events are shown in Table 4. The weather type favorable for yellow sand build-up in eastern Asia, the representative weather type, showed two clusters(cluster 1 and 2) at 1000 and 850 hPa, while one(cluster 2) was shown at 500 and 300 hPa. In case of the yellow sand events, about 91 % and 81 % of the cluster 1 and 2 were shown at 1000 hPa and 850 hPa respectively. And about 60 % and 68 % of the cluster 2 were presented at 500 hPa and 300 hPa (Table 5).

Table 4. Selected yellow sand events and related weather types

Date	1000 hPa	850 hPa	500 hPa	300 hPa
1996. 3. 8	1	1	2	2
1996. 4. 17	1	1	2	2
1996. 4. 18	1	1	2	1
1996. 5. 2	2	3	1	1
1996. 5. 8	2	3	1	1
1996. 5. 9	2	3	1	1
1997. 3. 30	2	2	2	2
1998. 3. 28	2	2	2	2
1998. 3. 29	2	2	2	2
1998. 3. 30	2	2	2	2
1998. 4. 14	2	2	2	2
1998. 4. 15	2	2	2	2
1998. 4. 16	2	2	2	2
1998. 4. 17	2	2	2	2
1998. 4. 18	2	2	2	2
1998. 4. 19	3	2	3	2
1998. 4. 20	3	2	3	2
1998. 4. 21	2	3	3	2
1998. 4. 22	2	3	1	1
1998. 4. 28	3	2	3	3
1999. 4. 5	2	2	2	2
2000. 3. 19	1	1	2	2
2000. 3. 23	1	1	2	2
2000. 3. 24	1	1	1	2
2000. 3. 27	3	2	3	2
2000. 3. 28	2	2	2	2
2000. 3. 29	2	2	2	2
2000. 4. 7	1	1	2	2
2000. 4. 8	3	2	2	2
2001. 3. 3	2	2	2	2
2001. 3. 4	1	2	2	2
2001. 3. 5	1	1	2	2
2001. 3. 6	1	1	2	2
2001. 3. 7	2	1	2	2
2001. 3. 20	2	2	3	2
2001. 3. 21	2	2	1	2
2001. 3. 22	2	2	3	1
2001. 3. 23	2	2	3	3
2001. 3. 24	2	2	3	3
2001. 3. 25	2	2	3	2
2001. 4. 9	1	2	2	2
2001. 4. 10	2	2	2	2
2001. 4. 11	1	1	2	2
2001. 4. 12	1	1	2	2
2001. 4. 13	2	3	1	2
2001. 4. 14	3	1	2	2

Table 4. (Continued)

Date	1000 hPa	850 hPa	500 hPa	300 hPa
2001. 4. 24	2	3	1	1
2001. 4. 25	3	3	3	3
2001. 4. 26	3	2	3	3
2001. 5. 16	2	2	3	3
2001. 5. 17	2	2	2	3
2001. 5. 18	2	2	2	3
2001. 5. 19	1	1	1	1

Fig. 1 shows the representative weather types in the yellow sand events in springtime depending on the isobaric surface over Korea. The dominant feature on 1000 hPa and 850 hPa was the continental outflow from China to Korea(Figs. 1a and b), and the intensified deep trough passage and cold advection on 500 hPa and 300 hPa(Figs. 1c and d). This trough was associated with surface low-pressure system centered at the near Korean peninsula accompanied with a cold front extending southeastward through the East Sea. The strong surface pressure gradient behind the front and strong meandering streams with upper-level troughs made it possible to bring yellow sand over Korea. Thus the yellow sand events occurred frequently when Korea was located between a ridge and a trough including the strong meandering streams at 500 hPa and 300 hPa, and these pressure patterns of the upper troposphere are linked to the lower level.

The analyses of the cluster and weather maps helped to clarify the synoptic weather system during the yellow sand events. In addition, anticyclonic subsidence may transport downwards the dust-rich air parcel, and intrude into the lower level depending on the isobaric surface over Korea. The representative weather type is one of the key elements in predicting the yellow sand event.

4. Case studies associated with the yellow sand events

The characteristics of the weather types have been examined for special days when the heavy yellow sand events occurred over Korea. And also, we observed that enhancements of yellow sand at ground monitoring sites in Korea mainly occur in springtime under these weather types of the

Table 5. The occurrence days of yellow sand along the isobaric surface in springtime. Values in parentheses indicate the percentages of the weather types in the yellow sand events. Total occurrence number of the weather types is 53.

	1000 hPa		850 hPa		500 hPa	300 hPa
Cluster 1	14(26.4%)	*48(90.6%)*	13(24.5%)	*43(81.1%)*	11(20.8%)	10(18.9%)
Cluster 2	34(64.2%)		30(56.6%)		*31(58.5%)*	*36(67.9%)*
Cluster 3	5(9.4%)		10(18.9%)		11(20.8%)	7(13.2%)

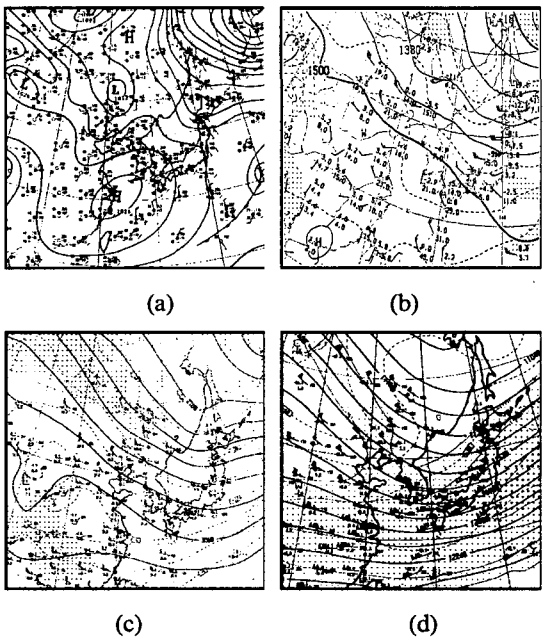

(a) (b)

(c) (d)

Fig. 1. The representative weather maps in the yellow sand events on 1000 hPa (a), on 850 hPa (b), on 500 hPa (c), and 300 hPa levels (d) over Korea in springtime.

intensified deep trough passage, cold advection, the continental outflow including surface high and low-pressure systems(Fig. 2). Fig. 2 shows the enhancements of yellow sand in the ground under weather maps on 6 and 7 March 2001. The wind flow of these weather maps is generally northwesterly over inland in Korea(see Fig. 1). In Fig. 2, the peak of concentration at Seoul presents at night on 6 March, and the peaks at Busan and Daegu(more than 500 $\mu g\ m^{-3}$) show in the daytime on 7 March 2001. This indicates that the time when the peak yellow sand concentration has occurred shows a delay at the sites downwind from inland to the coast in Korea. Thus we could know that yellow sand in the ground was also related to the long-range transport from China to Korea under the representative weather types.

To confirm this enhancement of yellow sand under those weather types, we simulated the origin by using HYSPLIT4 model and MM5 with the NCEP reanalysis data(2.5 ° × 2.5 °). In particular, the STE of yellow sand associated with the strong meandering stream was complemented with TOMS aerosol index and MM5 output data. This MM5 data set covers 60 km × 60 km resolution grids with 17 standard pressure surfaces between 1000 and 5 hPa. The size of these data is 84 × 84 with (1,1) = (90E, 60N) and (84, 84) = (140E, 10N), respectively. These model experiments may help to improve our understanding of yellow sand intrusions.

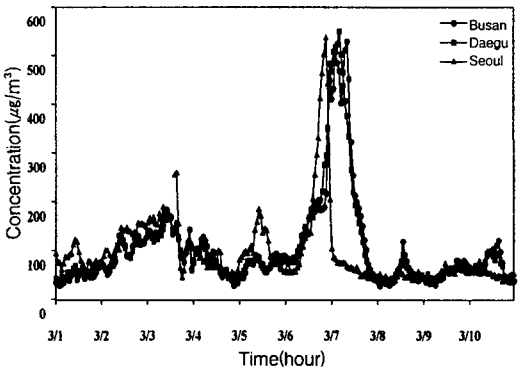

Fig. 2. Hourly surface concentrations of particulate matter(PM_{10}) observed at monitoring sites at Busan, Daegu, and Seoul in Korea during the periods of 10 days(1 ~ 10 March 2001).

In case studies with the numerical simulation, we confirmed the origin and transport of yellow sand with aerosol index of TOMS data, the pressure patterns between the upper and lower level, the

behavior of isentropic potential vorticity, and the estimation of backward trajectory.

Fig. 3 shows aerosol index derived from TOMS measurement on 5 and 7 March 2001. Yellow sand originates from Takla-Makan and Gobi deserts, Loess and Shan plateau and transported to Korea. It was assumed that there would be an intensive concentration over Korea on 7 March 2001. Based on the distribution of this aerosol index, we analyzed the vertical cross sections for isentropic potential vorticity(IPV) and vertical circulation and backward trajectories for tracing the flow of yellow sand in order to verify the mechanisms of the long-range transport in the yellow sand events.

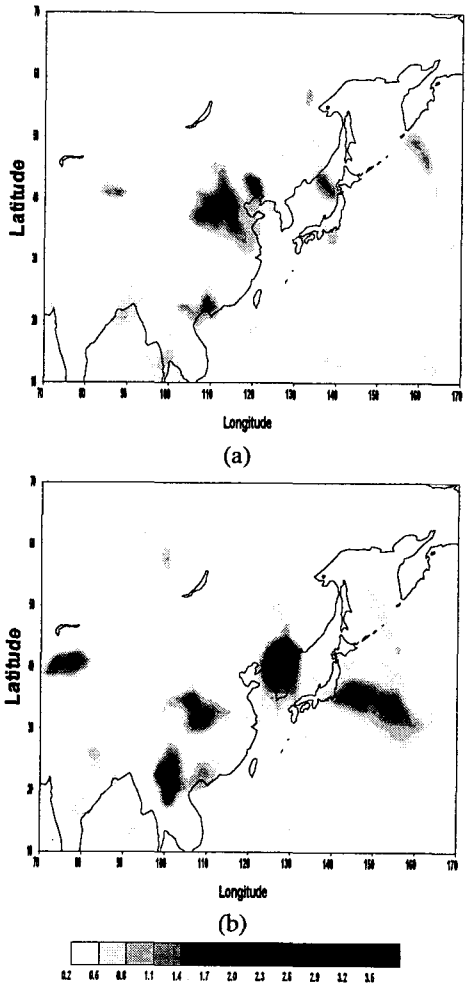

Fig. 3. The distribution of Aerosol index derived from TOMS measurement on 5 March (a) and on 7 March (b) 2001.

Fig. 4 shows the locations of vertical cross section, at A-B(17° N, 98° E - 50° N, 129° E), C-D(33.5° N, 90° E - 33.5° N, 140° E), and E-F (17° N, 129° E - 50° N, 129° E) to clarify the mechanisms and origin of the long-range transport of yellow sand. A-B cross section is for floating flows, C-D is for transporting flows, and E-F is for sinking flows. These vertical cross sections of three types along the longitude and latitude on 5 ~ 7 March 2001 are shown in Fig. 5. The vertical cross sections are presented diagonally in meteorological factors associated with downward transport of yellow sand in eastern Asia. Fig. 5a shows the floating flows in the source area of China at 1500 UTC on 5 March 2001, Fig. 5c shows the transporting flows of dust-rich air parcel from China to Korea at 0300 UTC on 6 March 2001, and Fig. 5d presents the sinking flows of air parcel over Korea at 2100 UTC on 6 March 2001. This shows that yellow sand occurs in the upper-level frontogenesis due to the polar and subtropical jet streams, and then the STE of air parcel including yellow sand occurs in downward motion of the secondary circulation or vertical wind shear caused by these two wind systems. This vertical motion develops around the entrance to a jet streak and lowers the stratospheric air on the polar side of the jet(Figs. 5d and e).

Thus yellow sand was floating in the source areas of China(Figs. 5a and b), transported toward Korea along the transport path of the meandering

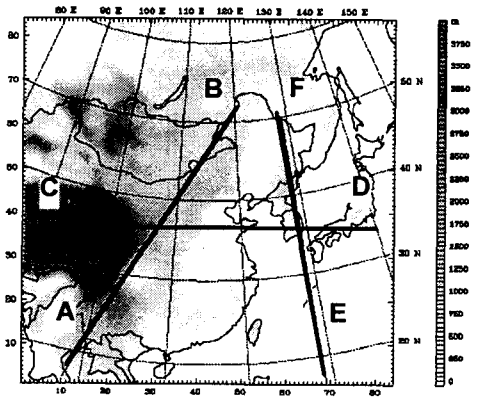

Fig. 4. Locations of vertical cross section. A(17° N, 98° E), B(50° N, 129° E), C(33.5° N, 90° ° E), D(33.5° N, 140° E), E(17° N, 129° E), and F(50° N, 129° E).

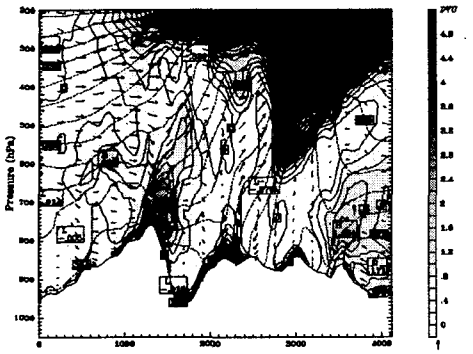

(a)

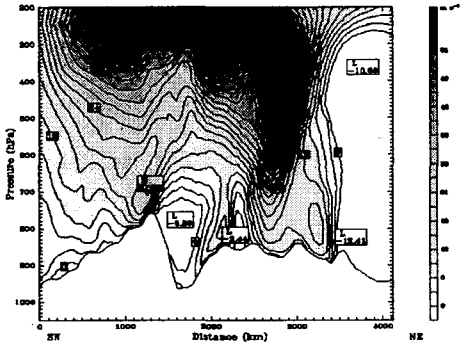

(b)

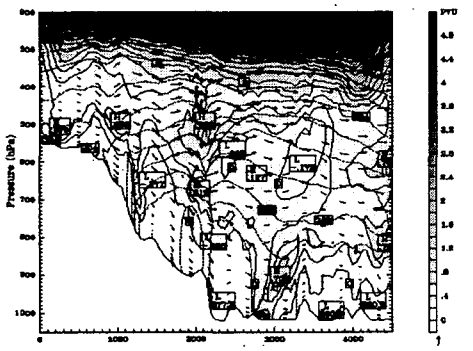

(c)

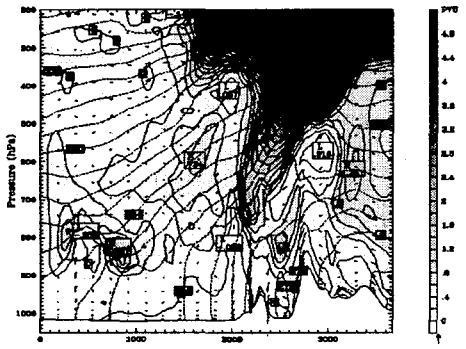

(d)

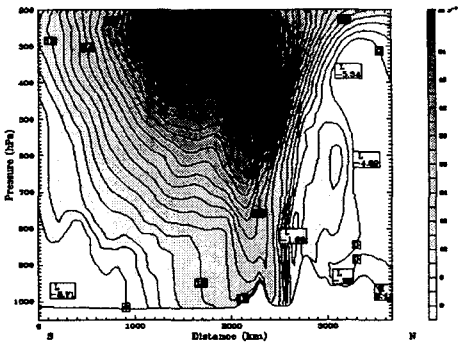

(e)

Fig. 5. Vertical cross sections for potential vorticity (a, c, d) and isotach(b, e) between A-B (a, b), C-D(c), E-F(d, e) (see Fig. 4) on 5-7 March 2001. Shown are isentropes (K, dashed lines), ageostrophic wind(m s^{-1}) and vertical wind (10^{-3} m s^{-1}), velocity(arrows), potential vorticity (1 PVU = 10^{-6} m^2 s^{-1} K kg^{-1}, solid lines), and isotach(m s^{-1}) simulated by MM5 using NCEP reanalysis data.

streams(Fig. 5c), and intruded into the lower troposphere near Korea(Figs. 5d and e) along the behavior of potential vorticity. We knew that the original area of yellow sand was located to the center of China with the variation of aerosol index (see Fig. 3).

Fig. 6 shows the two-day backward trajectories of the air mass arrived at Busan at 0000 UTC

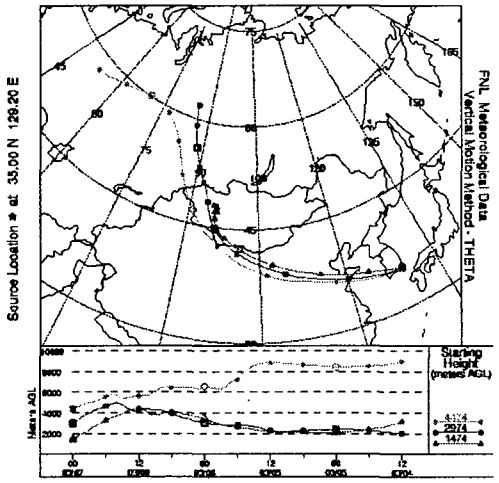

Fig. 6. Two-day backward trajectories of the air mass arrived at Busan at 0000 UTC on 7 March 2001 on the isentropic surface. AGL, above ground level.

on 7 March 2001. In particular, the 1500-m profile indicated that the source of yellow sand was from the Loess plateau and Gobi desert, at an elevation of approximately 4 km. The Hybrid Single-Particle Lagrangian Integrated Trajectory(HYSPLIT4) model[17] was employed for the backward trajectory analysis in this study.

Therefore, we can also know that the yellow sand events are transported from Loess plateau and Gobi desert, and are related to the long-range transport caused by the strong meandering streams in eastern Asia.

5. Conclusions

We have conducted studies on mechanisms of a long-range transport of Asian dust associated with the synoptic weather system and numerical simulation by using NCEP/NCAR reanalysis and TOMS data during the periods of 1996-2001. In cluster analysis, we concluded that three weather types at 1000 hPa, 850 hPa, 500 hPa, and 300 hPa levels were classified respectively. The dominant features at 1000 hPa and 850 hPa levels were the extending continental outflow from China to Korea, the deep trough passage and cold advection were shown and at 500 hPa and 300 hPa levels over Korea during the yellow sand events.

The case studies during the yellow sand events in 2001 has been analyzed with vertical cross sections of potential temperature, isentropic potential vorticity, and ageostrophic and vertical velocity to the upper trough/cut-off low using MM5. Yellow sand has occurred in the upper-level frontogenesis due to the polar jet and the subtropical jet, and then the STE of the dust-rich air parcel has occurred in the downward and upward movement of the secondary circulation or vertical wind shear caused by these two jets and surface high and low-pressure systems. From this we can conclude that yellow sand over and west of the cyclone over Korea partly originate from the strong meandering stream associated with the STE entering this region from the west, and also from air sinking by the surface high pressure system under the western side of the upper-level trough. On the other hand, yellow sand over and east of the cyclone originate from the strong meandering stream entering from the west and from air rising by the warm sector of the cyclone.

Based on this fundamental research, further studies to examine the episodic nature of yellow sand transport from Asia to North America and to predict the occurrence day of yellow sand through the specific cluster analysis of the weather types are necessary.

Acknowledgements

This research was supported by the Climate Environment System Research Center sponsored by the SRC program of Korea Science and Engineering Foundation.

References

[1] Murayama, N., 1988, Dust cloud "Kosa" from the east Asian dust storms in 1982-1988 as observed by the GMS satellite. Meteorol. Satell. Cent. Tech. Note 17, 1~8.

[2] Nakajima, T., M. Tanaka, M. Yamano, M. Shiobara, K. Arao, and Y. Nakanishi, 1989, Aerosol optical characteristics in the yellow sand events observed in May 1982 at Nagasaki, part II, Models. J. Meteorol. Soc. Jpn., 67, 279~291.

[3] Tanaka, M., M. Shiobara, T. Nakajima, M. Yamano, and K. Arao, 1989, Aerosol optical characteristics in the yellow sand events observed in May 1982 at Nagasaki, part I, Observations. J. Meteorol. Soc. Jpn., 67, 26 7~278.

[4] Gao, Y., Arimoto, R., Merril, J. T., Duce, R. A., 1992, Relationship between the dust concentration over eastern Asia and the remote North Pacific. J. Geophys. Res., 97, 9867~9872.

[5] Berntsen, T., S. Karlsdottir, and D. A. Jaffe, 1999, Influence of Asian emissions on the composition of air reaching the northwestern United States. Geophys. Res. Lett., 26, 2171~2175.

[6] Jaffe D. A., and Coauthors, 1999, Transport of Asian air pollution to North America. Geophys. Res. Lett., 26, 711~714.

[7] Husar, R. B., and Coauthors, 2001, The Asian dust events of April 1998. J. Geophys. Res.,

in press.

[8] Westphal, D. L., O. B. Toon, and T. N. Carlson, 1988, A case study of mobilization and transport of Sahara dust. J. Atmos. Sci., 45, 2145~2175.

[9] Tegen, I., A. A. Lacis, and I. Fung, 1996, The influence on climate forcing of mineral aerosols from disturbed soils. Nature, 380, 419~422.

[10] Marticorena, B., G. Bergametti, B. Aumount, Y. Callot, C. N'Doume, and M. Legrand, 1997, Modeling the atmospheric dust cycle, 2, Simulation of Saharan dust source. J. Geophys. Res., 102, 4387~4404.

[11] Kai, K., Y. Okada, O. Uchino, I. Tabata, H. Nakamura, T. Takasugi, and Y. Nikaidou, 1988, Lidar observation of a Kosa(Asian dust) over Tsukuba, Japan, during the spring of 1986. J. Meteorol. Soc. Jpn., 66, 457~472.

[12] Xiao, H., G. R. Carmichael, J. Durchenwald, D. Thornton, and A. Bandy, 1997, Long-range transport of Sox and dust in East Asia during the PEM B experiment. J. Geophys. Res., 102, 28589~28612.

[13] Wang, Z., H. Ueda, and M. Y. Huang, 2000, A deflation module for use in modeling long-range transport of yellow sand over east Asia. J. Geophys. Res., 105, 26947~26959.

[14] Joussaume, S., 1990, Three-dimensional simulations of the atmospheric cycle of desert dust particles using a general circulation model. J. Geophys. Res., 95, 1909~1941.

[15] Genthon, C., 1992, Simulation of desert dust and sea salt aerosols in Antarctica with a general circulation model of the atmosphere. Tellus, 44, 371~389.

[16] Holton, J. R., 1979, An Introduction to Dynamic Meteorology, Academic Press, New York, 167~169.

[17] Draxler, R. R. and Hess, G. D., 1998, An overview of the HYSPLIT 4 modeling system for trajectories, dispersion, and deposition. Aust. Meteorol. Mag., 47, 295~308.